Chapter 5
Piezoelectric Coefficients h_{ij}^*: New Opportunities to Improve Sensitivity

Abstract Piezoelectric coefficients h_{ij} characterise a link between an external mechanical strain applied to a sample and an electric field caused by the direct piezoelectric effect. At the converse piezoelectric effect, the piezoelectric coefficients h_{ij} characterise the link between a mechanical stress in the sample and electric displacement. Examples of the volume-fraction behaviour of the effective piezoelectric coefficients h_{ij}^* and the piezoelectric sensitivity associated with h_{ij}^* are analysed for the 2–2-type, 1–3-type and 0–3-type composites based on ferroelectrics. Relations between the piezoelectric coefficients h_{ij}^* and e_{ij}^* and some cases of the large anisotropy of h_{3j}^* are discussed for some composites.

In comparison to the piezoelectric coefficients d_{ij} and g_{ij}, the piezoelectric coefficients h_{ij} are considered and analysed in the literature on piezoelectric materials and applications to a small degree; see, for instance, monographs [1–3]. As is known from (1.11), the piezoelectric coefficients h_{ij} characterise the link between an external mechanical strain ξ_j that is applied to a sample and an electric field E_i caused by the direct piezoelectric effect. At the the converse piezoelectric effect, the piezoelectric coefficients h_{ij} are introduced to describe the link between a mechanical stress σ_j and an electric displacement D_i as shown in (1.10). In both the aforementioned links, the piezoelectric coefficients h_{ij} are accompanied by the minus sign, and it is an important feature of the piezoelectric effect [1, 3] described in terms of (1.10) and (1.11). The PS concerned with h_{ij} can be associated with a voltage between surfaces of the deformed sample, and this is important for piezoelectric sensor applications and monitoring the quality control of a production, surfaces of machine parts etc. [4, 5]. Equations (1.21) and (1.22) show that the piezoelectric coefficients d_{ij} and h_{ij} are linked by elastic and dielectric properties. The elastic properties are described by a fourth-rank tensor, and the dielectric properties are described by a second-rank tensor. Such an intricate character of the link between d_{ij} and h_{ij} in an anisotropic piezoelectric medium makes the problem of the microgeometry—PS relations more complicated and cannot lead to simple solutions concerning the effective properties of piezo-active composites. As follows from (1.21) and (1.23), the piezoelectric coefficients h_{ij} and e_{ij} are linked by the

V. Y. Topolov et al., *Piezo-Active Composites*, Springer Series
in Materials Science 271, https://doi.org/10.1007/978-3-319-93928-5_5

dielectric properties that are described by a second-rank tensor. This facilitates an analysis of the PS in terms of h_{ij} and by taking into account features of the behaviour of the piezoelectric coefficients e_{ij} (see Chap. 4). Like e_{ij}, the piezoelectric coefficients h_{ij} of the perovskite-type FCs [6] are divided into two groups. The first group contains materials with $h_{31} < 0$ and $h_{33} > 0$, and the second group contains materials with $h_{31} > 0$ and $h_{33} > 0$. For both these groups, the condition $h_{15} > 0$ holds. We remind that for poled FCs, the relation $\mathrm{sgn}e_{3j} = \mathrm{sgn}h_{3j}$ holds because of validity of (1.21) and (1.23).

In this chapter we describe examples of the PS of composites in terms of their effective piezoelectric coefficients h^*_{ij} and relations between h^*_{ij} and e^*_{ij}. Of specific interest are examples of the non-monotonic volume-fraction behaviour of h^*_{ij}, large values of $|h^*_{ij}|$ and large anisotropy of h^*_{ij} of some composites. We add that the main piezoelectric component of the studied composites is either the poled FC or domain-engineered SC.

5.1 2–2-Type Composites

The 2–2 composite structure shown in Figs. 2.1 and 2.2 is characterised by a system of alternating layers of two components, and at least one of them is piezoelectric, e.g. poled FC or SC. We assume that the OX_3 axis shown in Figs. 2.1 and 2.2 is the poling axis of the composite sample as a whole. In this section we discuss volume-fraction dependences of the piezoelectric coefficients h^*_{ij} in both series- and parallel-connected 2–2-type composites. Hereby we apply the matrix method [6] to determine the effective electromechanical properties of the 2–2-type composite (see details in Sect. 2.1.1).

The first example of the PS is concerned with a 2–2 series-connected composite based on FC. We remind that due to the poled FC layers and interfaces oriented perpendicular to the poling axis OX_3 (Fig. 2.1), the series-connected FC/polymer composite is described by ∞mm symmetry. In accordance with (1.21), the link between the piezoelectric coefficients e^*_{ij} and h^*_{ij} of such a composite is given by the following relations:

$$e^*_{31} = e^*_{32} = h^*_{31}\varepsilon^{*\xi}_{33},\ e^*_{33} = h^*_{33}\varepsilon^{*\xi}_{33} \text{ and } e^*_{15} = e^*_{24} = h^*_{15}\varepsilon^{*\xi}_{11}. \tag{5.1}$$

Relations between the piezoelectric coefficients e^*_{ij} and h^*_{ij} of the composite based on the PCR-7 M FC at large volume fractions of FC m are shown in Table 5.1. It is an original case of the composite for which conditions

$$|h^*_{31}| \gg h^*_{33} \text{ and } |h^*_{31}| \gg h^*_{15} \tag{5.2}$$

Table 5.1 Volume-fraction dependences of piezoelectric coefficients h_{ij}^* (in 10^8 V/m) and e_{ij}^* (in C/m^2) of 2–2 FC/polymer series-connected composites[a] at large volume fractions of FC m

Polymer	m	h_{31}^*	h_{33}^*	h_{15}^*	e_{31}^*	e_{33}^*	e_{15}^*
Composite based on the PCR-7 M FC							
Araldite	0.80	−9.63	2.80	3.18	−0.169	0.0492	7.14
	0.90	−10.0[a]	5.33	4.98	−0.349	0.186	11.1
	0.95	−9.40	8.63	6.93	−0.644	0.590	14.5
Elastomer	0.80	−10.6	0.466	0.256	−0.233	0.0102	0.704
	0.90	−11.7	1.02	0.501	−0.510	0.0443	1.52
	0.95	−12.0[b]	2.03	0.960	−1.03	0.173	2.96
Auxetic PE	0.80	−10.8	0.315	1.25	−0.109	0.00319	3.20
	0.90	−12.0	0.694	2.26	−0.242	0.0140	6.00
	0.95	−12.4[c]	1.41	3.77	−0.495	0.0564	9.49
Composite based on the modified $PbTiO_3$ (III) FC							
Araldite	0.80	−2.16	8.50	3.59	−0.0350	0.138	0.572
	0.90	−1.56	16.0	5.88	−0.0452	0.465	1.04
	0.95	−0.477	25.4	8.63	−0.0228	1.21	1.58
Elastomer	0.80	−3.77	1.44	0.272	−0.0750	0.0285	0.0440
	0.90	−4.01	3.13	0.536	−0.141	0.110	0.0973
	0.95	−3.80	6.20	1.04	−0.217	0.354	0.198
Auxetic PE	0.80	−4.15	0.970	1.36	−0.0402	0.00938	0.219
	0.90	−4.51	2.13	2.51	−0.0821	0.0389	0.451
	0.95	−4.43	4.32	4.35	−0.141	0.141	0.815

[a]See the schematic of the 2–2 series-connected composite in Fig. 2.1
[b]Diffuse min $h_{31}^* \approx -10.0 \times 10^8$ V/m is observed at $m = 0.87$–0.90
[c]Diffuse min $h_{31}^* \approx -12.0 \times 10^8$ V/m is observed at $m = 0.93$–0.96
[d]Diffuse min $h_{31}^* \approx -12.4 \times 10^8$ V/m is observed at $m = 0.94$–0.97

hold in specific ranges of m. This is accounted for by the orientation of the FC layers (see C1 in Fig. 2.1) with respect to the poling axis OX_3. At such an orientation, dielectric properties of the composite play the active role in the combination effect in accordance with (5.1), and the transverse PS concerned with h_{31}^* becomes dominating. However in a composite based on the modified $PbTiO_3$ FC, the piezoelectric coefficient h_{33}^* undergoes considerable changes (see Table 5.1), and conditions (5.2) become invalid. Such a performance is achieved due to positive signs of h_{3j} and a large anisotropy of h_{3j} of the FC component, see data in Table 1.6. In both the aforementioned 2–2 series-connected composites, changes in the piezoelectric coefficient h_{15}^* are appreciable in the relatively narrow volume-fraction range ($m = 0.80$–0.95, see Table 5.1) and depend on elastic properties of the polymer component.

The next important example of the PS is related to a 2–2 parallel-connected composite based on the [001]-poled KNNTL:Mn SC. This SC is of value as a piezoelectric material with large values of $|h_{3j}|$ at $|h_{31}| > h_{33}$: in accordance with experimental data by Huo et al. [7], $h_{31} = -1.29 \times 10^{10}$ V/m and $h_{33} = 1.06 \times 10^{10}$ V/m. These values are about two orders-of-magnitude larger than h_{3j} of the perovskite FCs listed in Table 1.6. Figure 5.1 shows that the piezoelectric coefficients h_{ij}^* of the parallel-connected composite obey conditions

$$h_{33}^* \gg |h_{31}^*|,\ h_{33}^* \gg |h_{32}^*|,\ h_{33}^* \gg h_{15}^*,\quad \text{and}\quad h_{33}^* \gg h_{24}^* \tag{5.3}$$

in specific volume-fraction ranges, including a region near diffuse max h_{33}^* (see curve 5 in Fig. 5.1). The system of the interfaces x_1 = const in the parallel-connected composite shown in Fig. 2.2 becomes an important factor that leads to the dominating longitudinal PS and validity of conditions (5.2). An even increase of the dielectric permittivity $\varepsilon_{33}^{*\xi}$ in the wide m range and the non-monotonic behaviour of the piezoelectric coefficient e_{33}^* (see curve 5 in Fig. 4.2 a) promote the large value of max h_{33}^* in accordance with (5.1). We note that the mutual arrangement of curves in Fig. 5.1 differs from the arrangement in Fig. 4.2a where the volume-fraction dependences of e_{ij}^* are represented for the same 2–2 composite. Such a difference is accounted for by the strong influence of dielectric properties of the composite on their piezoelectric coefficients h_{ij}^*.

5.2 1–3-Type Composites

In this section we discuss examples of the piezoelectric coefficients h_{ij}^* the 1–3 and related composites. In Fig. 2.11 where the typical 1–3 composite is shown, C1 is a component with a higher piezoelectric activity (e.g. poled FC or domain-engineered SC), and C2 is a component with a lower piezoelectric activity or a piezo-passive component.

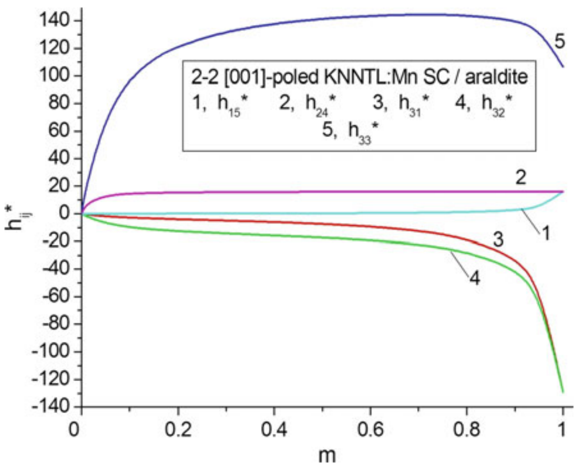

Fig. 5.1 Volume-fraction dependences of piezoelectric coefficients h_{ij}^* (in 10^8 V/m) of the 2–2 [001]-poled KNNTL: Mn SC/araldite parallel-connected composite. The schematic of the 2–2 parallel-connected composite is shown in Fig. 2.2

The first example is concerned with the 1–3 PZT-5 FC/araldite composite whose piezoelectric coefficients d^*_{3j}, e^*_{3j}, g^*_{3j}, and h^*_{3j} are shown in Fig. 4.3. To a large extent, changes in h^*_{3j} correlate with changes in d^*_{3j} and e^*_{3j} in the studied volume-fraction range. The longitudinal piezoelectric coefficient h^*_{33} of the 1–3 composite obeys conditions

$$h^*_{33} \gg \left|h^*_{31}\right| \text{ and } h^*_{33} \gg h^*_{15} \tag{5.4}$$

in the wide volume-fraction (m) range. Thus, the system of the aligned FC rods poled along the OX_3 axis (Fig. 2.11) would promote the considerable PS concerned with h^*_{33} of the 1–3 composite.

In the second example we show Fig. 5.2 where the piezoelectric coefficients h^*_{ij} of composites based on the KNNTL:Mn SC are represented at $0 < m < 1$. Changes in the polymer component lead to minor changes in the $h^*_{ij}(m)$ dependence. This dependence is formed at the active influence of the piezoelectric coefficients e^*_{ij} and dielectric permittivities $\varepsilon^{*\xi}_{pp}$ in accordance with (5.1). However these properties

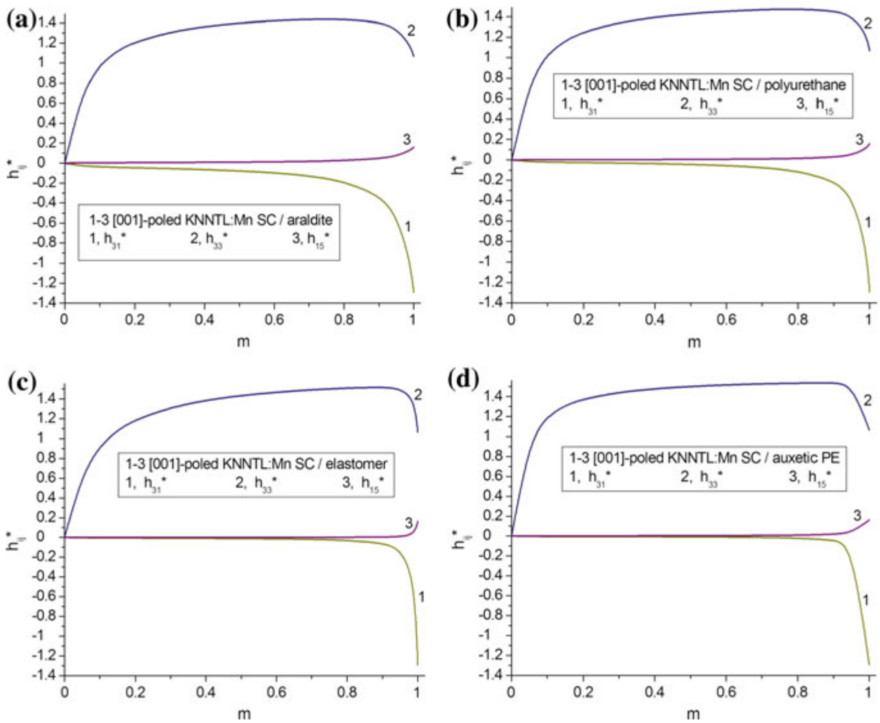

Fig. 5.2 Volume-fraction dependences of piezoelectric coefficients h^*_{ij} (in 10^{10} V/m) of 1–3 [001]-poled KNNTL:Mn SC/polymer composites. The schematic of the 1–3 composite is shown in Fig. 2.11

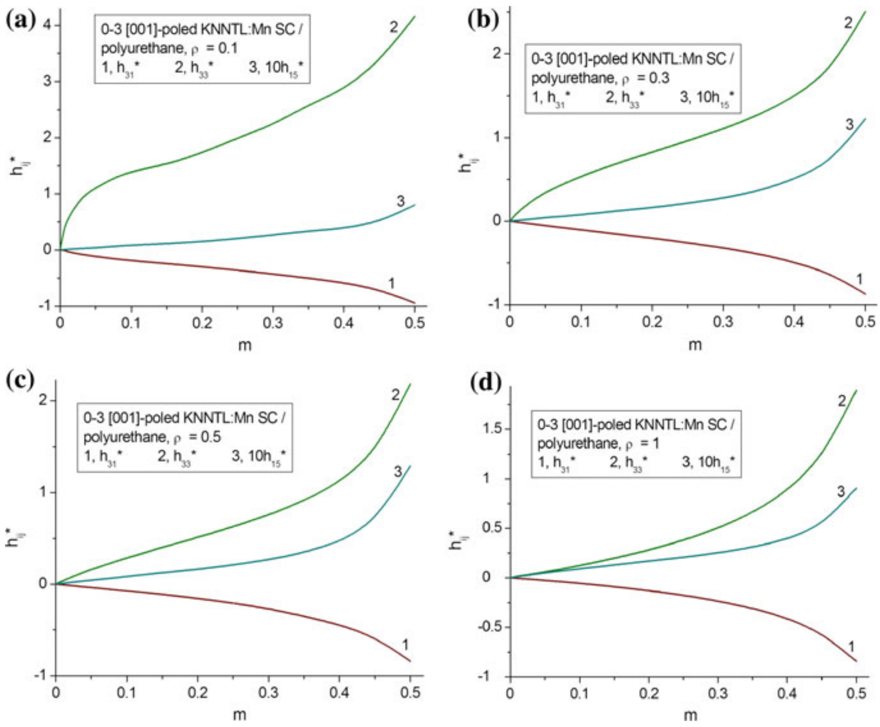

Fig. 5.3 Volume-fraction dependences of piezoelectric coefficients h_{ij}^{*} (in 10^{9} V/m) of the 0–3 [001]-poled KNNTL:Mn SC/polyurethane composite at ρ = const. The schematic of the 0–3 composite is shown in Fig. 2.28

undergo minor changes when replacing the polymer matrix in the 1–3 composite from Fig. 2.11. Changes in the polymer component do not lead to considerable changes of the value of max h_{33}^{*} (see curve 2 in Fig. 5.3) that is achieved at large volume fractions *m*. We add that this value is comparable to that found for the related 2–2 parallel-connected composite, see curve 5 in Fig. 2.2.

In the third example we consider relations between max e_{33}^{*} and max h_{33}^{*} which are found for a 1–3–0 composite with a porous polymer matrix. Such a composite is described in Sect. 2.2.4, see the schematic in Fig. 2.19. As follows from Table 5.2, changes in the porous polymer matrix would lead to tiny changes in max h_{33}^{*}, both in its value and location. The large values of the volume fractions *m* related to max h_{33}^{*} suggest that the elastic properties of the porous matrix would play a secondary role in forming the large piezoelectric coefficient h_{33}^{*}. It is also seen from Table 5.2 that max e_{33}^{*} is achieved at large (but smaller in comparison to max h_{33}^{*}) values of *m*. As a consequence, changes in max e_{33}^{*} at changes in the porous matrix become not very considerable. Like the 1–3 composites considered in the previous examples, the 1–3–0 composite based on the PMN–0.28PT SC is characterised by the large anisotropy of h_{3j}^{*}, and conditions (5.4) are valid in the wide *m* range.

Table 5.2 Maxima of piezoelectric coefficients h_{33}^* (in 10^{10} V/m) and e_{33}^* (in C/m^2) of the 1–3–0 [001]-poled PMN–0.28PT SC/porous araldite composite[a]

Porosity m_p in the matrix	Aspect ratio ρ_p = 0.01		Aspect ratio ρ_p = 1		Aspect ratio ρ_p = 100	
	max h_{33}^*	max e_{33}^*	max h_{33}^*	max e_{33}^*	max h_{33}^*	max e_{33}^*
0.1	0.431 (0.992)[b]	26.1 (0.891)	–[c]	25.5 (0.884)	0.434 (0.938)	26.6 (0.892)
0.2	0.432 (0.967)	27.1 (0.902)	0.431 (0.988)	26.1 (0.891)	0.435 (0.938)	27.0 (0.897)
0.3	0.433 (0.959)	27.9 (0.912)	0.432 (0.971)	26.8 (0.899)	0.435 (0.939)	27.4 (0.903)

[a]See the schematic of the composite in Fig. 2.19
[b]The volume fraction of SC m that is related to the maximum value is given in parentheses
[c]Monotonic $h_{33}^*(m)$ dependence

5.3 0–3-Type Composites

The 0–3 composite shown in Fig. 2.28 consists of the large matrix reinforced by the spheroidal inclusions (either FC or SC), and the poling axis of the composite as a whole is OX_3. We assume that the shape of each inclusion is described by (2.13) in the axes of the rectangular co-ordinate system ($X_1X_2X_3$), semi-axes of each inclusion are a_1, $a_2 = a_1$ and a_3, and its aspect ratio is defined as $\rho = a_1/a_3$. As in Sect. 2.4, we assume that the composite is characterised by the regular distribution of the spheroidal inclusions in the matrix. In this section we consider the PS of some 0–3-type composites whose electromechanical properties are evaluated by means of the FEM.

Graphs in Fig. 5.3 suggest that in a case of prolate SC inclusions poled along [001] ‖ OX_3, the piezoelectric coefficient h_{33}^* obeys conditions (5.4), i.e., the longitudinal PS is dominating. However for the [001]-poled KNNTL:Mn SC, $h_{33} = 1.06 \times 10^{10}$ V/m [7] that is a few times larger than h_{33}^* predicted for the 0–3

Table 5.3 Aspect-ratio (ρ) and volume-fraction (m) dependences of piezoelectric coefficients h_{ij}^* (in 10^9 V/m) and e_{ij}^* (in C/m^2) of the 0–3–0 [001]-poled PMN–0.33PT SC/porous PMN–0.35PT FC[a] composite

ρ	m	h_{31}^*	h_{33}^*	h_{15}^*	e_{31}^*	e_{33}^*	e_{15}^*
0.1	0.1	−0.129	1.24	0.922	−1.72	16.5	8.80
	0.3	−0.180	1.49	0.899	−2.13	17.4	9.24
	0.5	−0.251	1.82	0.875	−2.58	18.3	9.54
0.3	0.1	−0.132	1.24	0.922	−1.78	16.5	8.89
	0.3	−0.187	1.50	0.897	−2.27	17.5	9.22
	0.5	−0.262	1.83	0.872	−2.73	18.4	9.52
0.5	0.1	−0.135	1.24	0.920	−1.84	16.5	8.87
	0.3	−0.197	1.50	0.894	−2.42	17.5	9.19
	0.5	−0.277	1.84	0.868	−2.87	18.4	9.48

[a]The matrix is a poled FC medium with spherical air pores at porosity m_p = 0.3. The SC component is represented by a system of aligned spheroidal inclusions that are distributed in the porous FC matrix

composite, see curve 2 in Fig. 5.3. On increasing the aspect ratio ρ of the SC inclusion, the piezoelectric coefficient h_{33}^* becomes smaller at m = const. The similar decrease is also typical of the piezoelectric coefficient e_{33}^* as seen, for instance, from Table 4.6. It should be added that increasing the aspect ratio ρ does not lead to considerable changes in h_{31}^* and h_{15}^* of the composite, see curves 1 and 3 in Fig. 5.3. Thus, the isolated aligned piezoelectric inclusions in the 0–3 composite can influence its piezoelectric coefficients h_{ij}^* to a restricted degree.

The final example of the PS is concerned with a 0–3–0 composite wherein spheroidal SC inclusions are surrounded by a porous FC matrix. The performance of such a composite was discussed briefly in Sect. 4.3. We assume that each pore in the matrix of the 0–3–0 composite has the spherical form and radius being much smaller than the semi-axes of the inclusion a_1 and a_3. The composite sample as a whole is poled along the OX_3 axis. Data in Table 5.3 show that the correlation between the piezoelectric coefficients h_{3j}^* and e_{3j}^* is observed: we see the increase of $|h_{3j}^*|$ and $|e_{3j}^*|$ on increasing the volume fraction of SC m. Like e_{33}^*, the piezoelectric coefficient h_{33}^* takes almost equal values at m = const and various aspect ratios ρ, see the 4th column of Table 5.3. We observe validity of the inequality

$$h_{33}^* \gg |h_{31}^*| \tag{5.5}$$

in wide m ranges, and the value of the piezoelectric coefficient h_{15}^* remains comparable to the h_{33}^* value. Such a performance of the 0–3–0 composite can be concerned with specifics of an electromechanical interaction of its piezoelectric components. In contrast to h_{3j}^*, the piezoelectric coefficient h_{15}^* decreases on increasing m and e_{15}^*, see the 5th and 8th columns of Table 5.3. As follows from (5.1), the piezoelectric coefficients h_{15}^* and e_{15}^* are linked by the dielectric permittivity $\varepsilon_{11}^{*\xi}$, and its influence on h_{15}^* increases on increasing the volume fraction m.

5.4 Conclusion

This chapter has been devoted to the analysis of the piezoelectric coefficients h_{ij}^* and related PS of some two- and three-component composites. The following connectivity patterns can be of interest when studying h_{ij}^* and ways to improve the PS: 1–3, 1–3–0, 2–2, 0–3, and 0–3–0. Changes in the volume fraction of the piezoelectric component and microgeometry of the composite lead to changes in h_{ij}^* and their anisotropy, however these changes are different for different connectivity patterns and depend on the main piezoelectric component of the composite. Examples of validity of conditions (5.2)–(5.5) are discussed for a few composites, and features of the volume-fraction and aspect-ratio behaviour of the piezoelectric coefficients h_{ij}^* are interpreted by taking into account microgeometry and properties of components. Of specific interest is the PS of the 2–2 and 1–3 composites based on the KNNTL:

Mn SC: in these composites values of $h_{33}^{*} \sim 10^{10}$ V/m are achieved in wide volume-fraction ranges due to the large piezoelectric coefficient h_{33} of the SC component. In composites based on relaxor-ferroelectric SCs values of $h_{33}^{*} \sim (10^{8}–10^{9})$ V/m are achieved.

The PS associated with the piezoelectric coefficients h_{ij}^{*} can be taken into account in sensor applications, especially at the direct piezoelectric effect, when the electric field is caused by the mechanical strain of the sample.

References

1. Zheludev IS (1971) Physics of crystalline dielectrics. Vol 2: Electrical properties. Plenum, New York
2. Jaffe B, Cook WR, Jaffe H (1971) Piezoelectric ceramics. Academic Press, London
3. Ikeda T (1990) Fundamentals of piezoelectricity. Oxford University Press, Oxford, New York, Toronto
4. Steinem C, Janshoff A (eds) (2007) Piezoelectric sensors. Springer, Berlin, Heidelberg
5. Sharapov V (2011) Piezoceramic sensors. Springer, Heidelberg, Dordrecht, London, New York
6. Topolov VYu, Bowen CR (2009) Electromechanical properties in composites based on ferroelectrics. Springer, London
7. Huo X, Zhang R, Zheng L, Zhang S, Wang R, Wang J, Sang S, Yang B, Cao W (2015) (K, Na, Li) (Nb, Ta)O_3: Mn lead-free single crystal with high piezoelectric properties. J Am Ceram Soc 98:1829–1835